American Mineralogist, Volume 101, pages 1691–1695, 2016

Detection of liquid H_2O in vapor bubbles in reheated melt inclusions: Implications for magmatic fluid composition and volatile budgets of magmas?

Rosario Esposito[1,2,*], Hector M. Lamadrid[3], Daniele Redi[4], Matthew Steele-MacInnis[5], Robert J. Bodnar[3], Craig E. Manning[1], Benedetto De Vivo[2], Claudia Cannatelli[2,6], and Annamaria Lima[2]

[1]Earth, Planetary and Space Sciences, UCLA, 595 Charles Young Drive East, Los Angeles, California 90095-1567, U.S.A.
[2]DISTAR, Università Federico II, Via Mezzocannone 8, Napoli, 80134, Italy
[3]Department of Geosciences, Virginia Tech, 4044 Derring Hall, Blacksburg, Virginia 24061, U.S.A.
[4]BiGea, Dipartimento di Scienze Biologiche, Geologiche ed Ambientali, Via di Porta San Donato 1, 40126, Bologna, Italy
[5]Department of Geosciences, University of Arizona, Tucson, Arizona 85721, U.S.A.
[6]Department of Geology and Andean Geothermal Center of Excellence (CEGA), Universidad de Chile, Santiago 8370450, Chile

Abstract

Fluids exsolved from mafic melts are thought to be dominantly CO_2-H_2O ± S fluids. Curiously, although CO_2 vapor occurs in bubbles of mafic melt inclusions (MI) at room temperature (*T*), the expected accompanying vapor and liquid H_2O have not been found. We reheated olivine-hosted MI from Mt. Somma-Vesuvius, Italy, and quenched the MI to a bubble-bearing glassy state. Using Raman spectroscopy, we show that the volatiles exsolved after quenching include liquid H_2O at room *T* and vapor H_2O at 150 °C. We hypothesize that H_2O initially present in the MI bubbles was lost to adjacent glass during local, sub-micrometer-scale devitrification prior to sample collection. During MI heating experiments, the H_2O is redissolved into the vapor in the bubble, where it remains after quenching, at least on the relatively short time scales of our observations. These results indicate that (1) a significant amount of H_2O may be stored in the vapor bubble of bubble-bearing MI and (2) the composition of magmatic fluids directly exsolving from mafic melts at Mt. Somma-Vesuvius may contain up to 29 wt% H_2O.

Keywords: Raman spectroscopy, Mt. Somma-Vesuvius, volatile solubility, mafic melt, sulfur budget, melt inclusion, fluid inclusion, heating experiments

Introduction

Melt inclusions (MI) are aliquots of melt trapped in phenocrysts during crystallization of magmas. MI analyses potentially allow characterization of the volatile contents of pre-eruptive silicate melts. Typically, concentrations of volatiles such as H_2O, CO_2, and S are measured in the glass phase in quenched MI and compared to experimentally determined solubility models to deduce the composition of a coexisting vapor phase (Métrich and Wallace 2008 and references therein). However, recent studies have emphasized that, after entrapment, most of the CO_2 may be transferred from the melt or glass to a coexisting vapor bubble within the MI (e.g., Esposito et al. 2011), as a result of processes such as post-entrapment crystallization (Steele-MacInnis et al. 2011) or differential thermal contraction (Moore et al. 2015 and references therein). In fact, bubbles in MI may contain more CO_2 (by mass) than the coexisting glass phase (Anderson and Brown 1993; Esposito et al. 2011; Hartley et al. 2014; Moore et al. 2015; Wallace et al. 2015). Thus, it is necessary to understand the partitioning of volatiles between melt (or glass) and bubbles during MI cooling as part of the characterization of pre-eruptive volatile systematics (e.g., Kamenetsky et al. 2002; Lowenstern 1995).

H_2O may be abundant in mafic melts and should also be partitioned into any MI bubbles that form. However, reports of condensed, liquid H_2O are chiefly in MI hosted by quartz in felsic plutonic systems (e.g., Frezzotti 2001; Harris et al. 2003; Zajacz et al. 2008). Several studies have commented on the non-detection of H_2O in bubbles within felsic and mafic melt inclusions in volcanic rocks. For instance, Lowenstern et al. (1991) reported CO_2 vapor in the bubbles of reheated MI hosted in quartz from Pantelleria (Italy), and stated that H_2O was likely present in the bubble, but "*the lack of a liquid phase in the bubble and negligible H_2O vapor peaks in the IR spectra indicated that it was subordinate to CO_2.*" Yang and Scott (1996) and Kamenetsky et al. (2002, 2001) also found that the main volatile component of MI bubbles was CO_2, and echoed Lowenstern et al. (1991) in stating that although H_2O was likely present, it was not detected. It is important to note that Kamenetsky et al. (2002) detected H_2O as a component of gypsum, nahcolite, and silicate crystals found at bubble-glass interfaces. Moore et al. (2015) suggested that the "missing" H_2O could reflect nuances of spectroscopic detection of H_2O, particularly given that H_2O-CO_2 fluids would likely separate into an H_2O-rich liquid and CO_2-rich vapor at ambient conditions. Anderson (1991) suggested that H_2O could be present in devitrified glass surrounding bubbles.

Based on the various results and interpretations described above, H_2O is expected to be a major component of magmatic

* E-mail: r.esposito@epss.ucla.edu

0003-004X/16/0007–1691$05.00/DOI: http://dx.doi.org/10.2138/am-2016-5689

fluids contained in bubbles that form in MI during cooling, but direct evidence of liquid or vapor H_2O in bubbles in olivine-hosted, basaltic MI has not, to our knowledge, been reported. In this study, we hypothesized that liquid H_2O may be recognized in "fresh" bubbles generated by laboratory re-heating and quenching of MI. Naturally glassy MI were heated to conditions at which the silicate component of the MI was fully molten. With subsequent quenching, a glass and bubble would be produced, and liquid H_2O in the bubble, if present, could be detected because it would have little time to interact with the surrounding glass.

Materials and methods

Sixteen olivine phenocrysts were selected from lavas and pumices produced during mild effusive events and explosive Plinian eruptions of Mt. Somma-Vesuvius, Italy, between >33 ka and AD 1631 (Supplement A[1]). Bulk-rock compositions of the samples studied span a wide range, and correspond to samples reported by Ayuso et al. (1998). Lava samples are slightly Si-undersaturated and plot at the boundary between the trachybasalt/shoshonite fields on the TAS diagram (Le Bas et al. 1986). Pumice samples show a higher degree of Si undersaturation and plot in the phonotephrite, tephriphonolite, and phonolite fields. The olivines selected for this study span a wide compositional range from 68 to 90 mol% forsterite (Redi 2014). We identified MI based on petrographic analysis. Particular care was taken to select MI not showing decrepitation or fractures intersecting the MI. We performed heating experiments using a Vernadsky heating stage (Sobolev et al. 1980). The average duration of the heating experiments was 17 min (Supplement B[1]), but MI were not heated for more than 9 min at T >800 °C. The 16 phenocrysts contained bubble-bearing MI after quenching from the maximum T (1143–1238 °C; Fig. 1 and Table DR1[1]). After rapid quenching, the bubbles were examined for evidence of volatile components (CO_2, H_2O, etc.) in the exsolved magmatic fluid. The MI were analyzed by Raman spectroscopy (Supplement B[1]). The Raman signal corresponding to hydroxyl ions and molecular H_2O (H_2O/OH) dissolved in the glass (Figs. 2 and 3) is clearly discernible from the signals of both H_2O liquid at the glass/bubble interface (Fig. 3) and the H_2O in the H_2O-CO_2 vapor phase at >100 °C. The density of CO_2 in the vapor phase was calculated from the splitting of the CO_2 Fermi diad (Supplement B[1]).

Some vapor bubbles were analyzed by Raman spectroscopy at high T (up to 150 °C) to test for the presence of H_2O in the bubbles (Supplement B[1]). To estimate concentrations of H_2O and CO_2 in the magmatic vapor phase, we compared the relative peak areas of H_2O and CO_2 in the spectra acquired at 150 °C (Supplement B[1]). In addition, five freezing/heating experiments were performed on MI bubbles (Supplement B[1]).

Results

Twenty MI selected for this study were examined petrographically before, during, and after the heating experiments (Table DR1). MI varied from slightly crystallized to highly crystallized (e.g., Fig. 1). Details of the microthermometric behavior of MI are reported in Supplement C[1]. We did not heat the MI until the bubble was completely dissolved, because our aim was to quench a vapor bubble in thermal equilibrium with a silicate melt at maximum T to study its vapor constituents. The olivine phenocrysts were held at maximum T (1143–1238 °C) for ~3 min to attain thermal equilibrium. Immediately prior to quenching, the MI contained silicate liquid plus a minute vapor bubble. After quenching to room T, the MI contained glass plus a bubble.

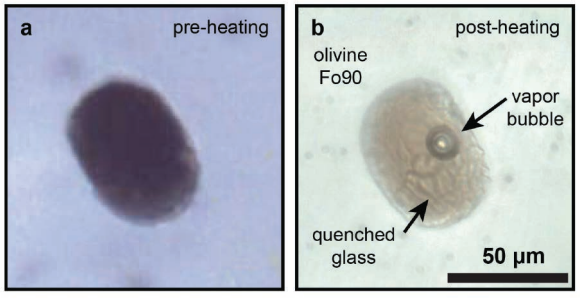

Figure 1. Photomicrographs of MI hosted in olivine from the Pompeii eruption (AD 79). (**a**) Crystallized MI "as found" (before heating experiment). (**b**) Bubble-bearing MI after quenching following heating experiment. (Color online.)

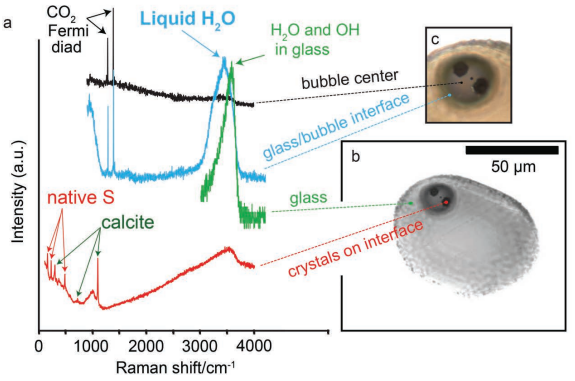

Figure 2. Raman analyses of MI hosted in olivine SCL14-D92-3-1 from a Pre-Codola (>33 ka) lava. (**a**) Raman spectra obtained at different depths and position in the MI. Note the variation in H_2O peak intensity at the various depths (a.u. = arbitrary units). (**b**) Photomicrograph of the MI showing the hexagonally shaped, dark solids at the glass/bubble interface. (**c**) Enlargement of the bubble in **b**. (Color online.)

When the laser beam of the Raman microprobe was focused in the center of the bubble, CO_2 was detected in all cases. The density of CO_2 ranged from 0.04 to 0.14 g/cm^3 with one outlier (Table DR1[1]). No H_2O was detected in the vapor at room T. The bubbles were also analyzed at the glass-bubble interface. At the upper interface, sub-hexagonal crystals and dark flakes of calcite (in four bubbles) or calcite plus native sulfur (in three bubbles) were observed and analyzed (Fig. 2b; Table DR1). We did not observe these crystal aggregates at high T. We also detected gypsum at the glass/bubble interface of one vapor bubble (P1-D49-2-7; Fig. C1[1] and Table DR1[1]). After focusing on the calcite ± native sulfur aggregates, the laser was focused ~1 µm below or beside the crystalline aggregates (Fig. 2). At this position, five MI also showed evidence of liquid H_2O at the glass-bubble interface (Table DR1). Some Raman spectra at the glass-bubble interface indicated the coexistence of carbonates ± native sulfur, H_2O, and CO_2 (Fig. 2a). In six H_2O-bearing MI, the presence of H_2O and CO_2 was confirmed by microthermometry. Five bubble-bearing MI analyzed by microthermometry showed first melting ranging from –57.1 to –56.0 °C (Table DR1), close to the triple point of CO_2 (–56.6 °C), suggesting that the vapor is nearly pure CO_2. A second phase change was observed at –2 to +8 °C in four out of the five bubbles, likely representing melting of H_2O-ice or CO_2-H_2O clathrate.

Three H_2O-bearing samples were heated to 150 °C after quenching. At this temperature, liquid H_2O was no longer observed and the vapor in the bubbles showed the sharp O-H stretching band

[1]Deposit item AM-16-75689, Supplemental Material. Deposit items are free to all readers and found on the MSA web site, via the specific issue's Table of Contents (go to http://www.minsocam.org/MSA/AmMin/TOC/).

of H_2O vapor (Frezzotti et al. 2012) at ~3647 cm^{-1} (Fig. 3). This indicates that the H_2O occurring as liquid at room *T* had dissolved into the CO_2-rich vapor phase at higher *T*.

The molar fractions of H_2O and CO_2 were estimated from the relative Raman peak areas, normalized according to the relative scattering efficiencies (Burke 2001). For inclusion LFL2-D44-3-2 (Avellino eruption), two analyses at two focal depths within the bubble yielded H_2O concentrations of 20 ± 12 mol% and 30 ± 21 mol% H_2O.

Discussion and implications

Bubbles in MI may contain significant proportions of the total CO_2 in the inclusions (Anderson and Brown 1993; Esposito et al. 2011; Hartley et al. 2014; Moore et al. 2015; Wallace et al. 2015), but evidence for the expected H_2O has been hitherto lacking. Our results demonstrate that bubbles in reheated MI from Mt. Somma-Vesuvius show evidence of H_2O and S, in addition to CO_2. At ambient *T*, H_2O is present as a thin liquid film at the bubble-glass interface, and S is present in minute daughter crystals. The presence of H_2O in reheated bubbles raises the possibility that the bubble volatile phase may initially have been H_2O rich.

Based on the Raman spectroscopic data and constraints from previous studies (Belkin and De Vivo 1993; Marianelli et al. 2005), we estimated that the thickness of the liquid H_2O film contained in the MI bubbles ranges from ~0.01 to 0.51 μm and, thus, in all cases, the liquid H_2O annulus would be optically undetectable (see Supplement D[1] and Table DR2[1]). In this study we did not attempt to establish the bulk H_2O content of the MI, but previous results can be used as a guide (e.g., Webster et al. 2001).

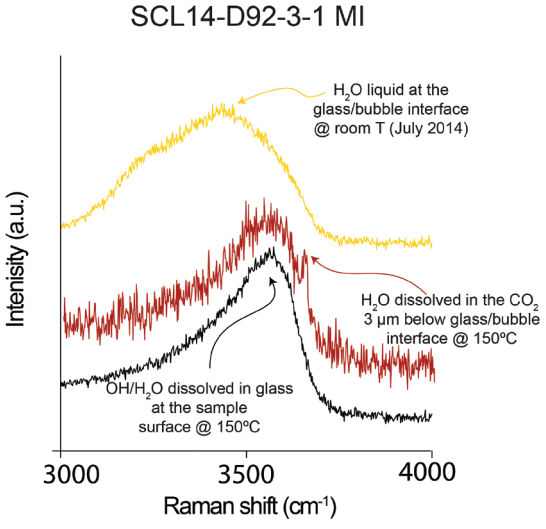

Figure 3. Raman spectra collected from the vapor bubble in MI SCL14-D92-3-1 at different conditions and depths. The yellow spectrum was collected from the MI at room temperature while focusing the laser at the glass/bubble interface in July 2014 and shows the H_2O fluid band. The black spectrum was collected at 150 °C while focusing the laser in the glass in the MI and shows the OH and H_2O band at ~3550 cm^{-1}. Note the difference between the peak positions of liquid H_2O in the synthetic fluid inclusion and at the glass/bubble interface and those of hydroxyl and molecular water dissolved in the silicate glass. The red spectrum represents the H_2O band collected at 150 °C while focusing the laser at the glass/bubble interface in the MI. Notice that the H_2O band of liquid water was not observed at 150 °C, while a peak at ~1650 cm^{-1} was only detected at this temperature (a.u. = arbitrary units). (Color online.)

Sample MI SCL14-D92-3-1 (Fig. 2) is representative of lava samples studied by Webster et al. (2001). If we assume that the concentration of H_2O ranges from 20 to 60 mol%, the thickness of liquid H_2O film at the glass/bubble interface of MI SCL14-D92-3-1 is 0.04–0.23 μm (Table DR2[1]). The amount of H_2O stored in this bubble represents between 3 and 16% of the total amount of H_2O in the melt that was trapped in the MI if we assume that the H_2O content of the original trapped melt is 0.3 wt%, consistent with the lowest H_2O content reported by Webster et al. (2001, see their Table 1). Webster et al. (2001) give an upper bound of 5 wt% H_2O. Assuming this value, the amount of H_2O stored in the bubble of this MI is insignificant, and is the reason for the query in the title of this letter. In general, the amount of H_2O in the bubbles of bubble-bearing MI may be significant for (1) relatively low H_2O concentration of the originally trapped melt, (2) relatively high mol% H_2O in the fluid, and (3) relatively large vapor bubbles. In addition, a constant volume percent bubble with a 1 μm thick rim of liquid H_2O represents an increasingly larger proportion of the total H_2O in the MI as MI size decreases. As an example, consider a bubble with 85 mol% H_2O, condensed as a liquid H_2O film that is 1 μm thick (thus not optically recognizable) and assuming CO_2 density is 0.14 g/cm^3. The H_2O in the bubble would represent 59% of the total H_2O in the MI if the H_2O concentration of the glass is 0.3 wt%, and assuming the bubble is 3 vol% of the MI.

The likely reason that H_2O has been overlooked in most MI studies is that in most MI, the H_2O originally in the vapor bubble is now contained in the surrounding glass phase via hydration (Anderson 1991; Parruzot et al. 2015). Devitrification and alteration of silicate glass in the presence of H_2O is a relatively fast process [~10^3 years at ambient *T* (Lee et al. 1974), ~days at >200 °C (Mazer et al. 1991)]. Thus, H_2O liquid would only be detected in vapor bubbles if the H_2O re-dissolves into the bubble when the MI is re-heated and then quenched. Even if the H_2O component was not incorporated into the glass via devitrification, it is unlikely that the thin film of liquid H_2O at the glass/bubble interface would be discernible because the resolution with an optical microscope is on the order of 1 μm, and the rims may be <<1 μm (Supplement D[1] and Table DR2). In these cases, it is important to investigate the glass/bubble interface for liquid ± solid(s). These interpretations are consistent with preliminary indications of H_2O liquid in shrinkage bubbles of olivine hosted MI from the San Cristóbal volcano in the Central American Volcanic Arc (Robidoux et al. 2015).

The results of this study also provide direct evidence of native S, in addition to H_2O, CO_2, carbonates, and sulfates in vapor bubbles in MI. The presence of S in the vapor bubble underscores the possibility that the original S concentration of the melt would be underestimated if only the S contained in the glass is considered. We estimate that the S in the bubbles ranges from 108 to 1192 ppm, comparable to the concentration of S reported by Webster et al. (2001), which ranged from 200 to 2900 ppm. Our calculation assumed that crystals at the glass-bubble interface are a mixture of calcite and native sulfur of various proportions, and that the H_2O/CO_2 molar ratio ranges from 0.25 to 1.5, and that these crystals are from 1 to 2 μm thick (Supplement D[1]). Thus, including the contribution of S in the bubble to the total S content of the MI could more accurately estimate the pre-eruptive S concentration

Table 1. Volatile budget of bubbles in MI (see text and Supplement D[1] for calculations)

MI	SCL14-D92-3-1	SCL14-D92-3-1	LFL2-D44-1-1	LFL2-D44-1-1	P1-D492-7	P1-D492-7	R6-D54-4-2	R6-D54-4-2
Eruption	Pre-Codola	Pre-Codola	Avellino	Avellino	Pompeii	Pompeii	AD 1631	AD 1632
	min	max	min	max	min	max	min	max
				Mass relative to Total MI (ppm)				
CO_2 vapor	774	774	788	788	380	380	330	330
CO_2 calcite	74	662	79	969	0	0	94	342
H_2O liquid	77	464	81	483	121	242	34	210
Native S	124	1116	132	1192	0	0	64	576
Gypsum S	0	0	0	0	108	216	0	0
Total	1049	3016	1080	3432	609	838	522	1458
Magmatic fluid composition	min	max	min	max	min	max	min	max
				Mass relative to vapor bubble (wt%)				
CO_2 wt%	35	88	34	89	45	45	32	87
H_2O wt%	4	27	4	27	20	29	3	26
S wt%	6	55	6	56	18	26	7	59

of silicate melts if the melt was originally trapped as single melt phase. We estimate that the composition of the C-O-H-S magmatic fluid exsolving from the mafic melts in this study is 32–89 wt% CO_2, 3–29 wt% H_2O, and 6–59 wt% S (Table 1; see Supplement D[1] for calculations).

An important consideration when evaluating the role of bubbles in the volatile contents of MI will be open system effects, such as hydrogen loss. Hydrogen loss during heating experiments may not significantly change the H_2O content of a MI if the experiment is on the order of a few minutes (Bucholz et al. 2013; Gaetani et al. 2012). The maximum time that the MI studied were held at $T > 800$ °C is 9 min. We calculated that change in the H_2O content of the MI during the experiments is <0.1 wt% if the starting H_2O concentration of MI was 4 wt% (see Supplement E[1] for more details). However, it is possible that H and Fe loss by diffusion occurred after trapping and before eruption (Danyushevsky et al. 2002) because the history of the MI from trapping to eruption is unknown.

In this study, we cannot establish if the melt inclusions were originally trapped as volatile-saturated or volatile-undersaturated melts, nor do we know whether bubbles were present at the time of MI trapping or formed later. We emphasize that the goal of this study was not to investigate the trapping conditions of the MI and the original magmatic vapor potentially trapped in the MI. Our goal was instead to use the MI as a natural laboratory where we were able to form a vapor bubble at magmatic T in thermal equilibrium with a silicate melt. The observation that reheated and quenched MI contain a silicate glass plus a fluid bubble indicates that a magmatic vapor phase exsolved from and coexisted with the melt prior to laboratory quenching because MI studied show a single bubble at maximum T before quenching. The bubbles in the MI investigated in the present study represent a magmatic volatile phase that exsolved from and was in equilibrium with silicate melt at temperatures and pressures appropriate for sub-volcanic environments, assuming that the bubbles did not lose or gain volatiles during quenching. At this stage, we cannot rule out possible modifications to the MI after trapping (e.g., H-loss). Thus, the volatiles in the vapor bubbles could be representative of the magmatic fluid coexisting with the melt beneath Mt. Somma-Vesuvius only *if* the MI trapped a volatile-saturated melt, the composition of the MI is unmodified, and the temperatures (and internal pressures in the inclusions) attained during heating experiments correspond to the MI trapping conditions. Violation of any of the above criteria would imply that the MI bubbles do not represent the magmatic vapor phase specific to Mt. Somma-Vesuvius.

Regardless of their origin, our results show that bubbles in MI should be carefully taken into account in any assessment of the volatile concentrations of MI in some magmatic systems. The direct detection of liquid H_2O in vapor bubbles in MI has several potential implications concerning magmatic fluids. For instance, the newly formed vapor bubbles in MI allow us to investigate the composition of the magmatic fluid directly exsolving from a natural melt. Raman analysis, coupled with freezing and heating studies, can be applied to investigate the volatile species and the composition of magmatic fluids. Also, one could investigate the rate at which the liquid H_2O reacts with the surrounding glass by conducting time-resolved Raman imaging analysis (e.g., Bartoli et al. 2013) at the glass/bubble interface following the formation of vapor bubbles during cooling of MI in the laboratory.

Acknowledgments

This work was supported by the 7/PON/ST/2012-4 Enerbiochem project to B. De Vivo. Partial funding for MI analysis was provided by PRIN2010PMKZX7 to C. Cannatelli. R. Esposito thanks E. Ammannito for discussions on peak fitting of the Raman spectra, and D. Moncada for help during heating/freezing experiments and Raman analysis at Virginia Tech. Funding was provided in part by the National Science Foundation (Grant Nos. EAR-1019770, Bodnar; EAR-1347987, Manning) and the Deep Carbon Observatory. We thank L. Danyushevsky for critical comments and help with heating experiments. We thank three anonymous reviewers for critical comments on an earlier version of this manuscript, A.J. Anderson, C. Bucholz, and M.L. Frezzotti for valuable comments that helped to improve this letter, and I. Swanson for editorial handling of this manuscript.

References cited

Anderson, A.T. Jr. (1991) Hourglass inclusions: theory and application to the Bishop Rhyolitic Tuff. American Mineralogist, 76, 530–547.

Anderson, A.T. Jr., and Brown, G.G. (1993) CO_2 contents and formation pressures of some Kilauean melt inclusions. American Mineralogist, 78, 794–803.

Ayuso, R.A., De Vivo, B., Rolandi, G., Seal, R.R. II, and Paone, A. (1998) Geochemical and isotopic (Nd–Pb–Sr–O) variations bearing on the genesis of volcanic rocks from Vesuvius, Italy. Journal of Volcanology and Geothermal Research, 82, 53–78.

Bartoli, O., Cesare, B., Poli, S., Bodnar, R.J., Acosta-Vigil, A., Frezzotti, M.L., and Meli, S. (2013) Recovering the composition of melt and the fluid regime at the onset of crustal anatexis and S-type granite formation. Geology, 41, 115–118.

Belkin, H.E., and De Vivo, B. (1993) Fluid inclusion studies of ejected nodules from plinian eruptions of Mt. Somma-Vesuvius. Journal of Volcanology and Geothermal Research, 58, 89–100.

Bucholz, C.E., Gaetani, G.A., Behn, M.D., and Shimizu, N. (2013) Post-entrapment modification of volatiles and oxygen fugacity in olivine-hosted melt inclusions. Earth and Planetary Science Letters, 374, 145–155.

Burke, E.A. (2001) Raman microspectrometry of fluid inclusions. Lithos, 55, 139–158.

Danyushevsky, L.V., McNeill, A.W., and Sobolev, A.V. (2002) Experimental and petrological studies of melt inclusions in phenocrysts from mantle-derived magmas: an overview of techniques, advantages and complications. Chemical Geology, 183, 5–24.

Esposito, R., Bodnar, R.J., Danyushevsky, L., De Vivo, B., Fedele, L., Hunter, J., Lima, A., and Shimizu, N. (2011) Volatile evolution of magma associated with the Solchiaro Eruption in the Phlegrean Volcanic District (Italy). Journal of Petrology,

52, 2431–2460.
Frezzotti, M.-L. (2001) Silicate-melt inclusions in magmatic rocks: applications to petrology. Lithos, 55, 273–299.
Frezzotti, M.L., Tecce, F., and Casagli, A. (2012) Raman spectroscopy for fluid inclusion analysis. Journal of Geochemical Exploration, 112, 1–20.
Gaetani, G.A., O'Leary, J.A., Shimizu, N., Bucholz, C.E., and Newville, M. (2012) Rapid reequilibration of H_2O and oxygen fugacity in olivine-hosted melt inclusions. Geology, 40, 915–918.
Harris, A.C., Kamenetsky, V.S., White, N.C., van Achterbergh, E., and Ryan, C.G. (2003) Melt inclusions in veins: linking magmas and porphyry Cu deposits. Science, 302, 2109–2111.
Hartley, M.E., Maclennan, J., Edmonds, M., and Thordarson, T. (2014) Reconstructing the deep CO_2 degassing behaviour of large basaltic fissure eruptions. Earth and Planetary Science Letters, 393, 120–131.
Kamenetsky, V.S., Binns, R.A., Gemmell, J.B., Crawford, A.J., Mernagh, T.P., Maas, R., and Steele, D. (2001) Parental basaltic melts and fluids in eastern Manus backarc Basin: implications for hydrothermal mineralisation. Earth and Planetary Science Letters, 184, 685–702.
Kamenetsky, V., Davidson, P., Mernagh, T., Crawford, A., Gemmell, J., Portnyagin, M., and Shinjo, R. (2002) Fluid bubbles in melt inclusions and pillow-rim glasses: High-temperature precursors to hydrothermal fluids? Chemical Geology, 183, 349–364.
Le Bas, M.J., Le Maitre, R.W., Streckeisen, A., and Zanettin, B.A. (1986) Chemical classification of volcanic rocks based on the total alkali-silica diagram. Journal of Petrology, 27, 745–750.
Lee, R., Leich, D., and Tombrello, T. (1974) Obsidian hydration profile measurements using a nuclear reaction technique. Nature, 250, 44–47.
Lowenstern, J.B. (1995) Applications of silicate-melt inclusions to the study of magmatic volatiles. Short Course Handbook, 23, 71–99.
Lowenstern, J.B., Mahood, G.A., Rivers, M.L., and Sutton, S.R. (1991) Evidence for extreme partitioning of copper into a magmatic vapor phase. Science, 252, 1405–1409.
Marianelli, P., Sbrana, A., Métrich, N., and Cecchetti, A. (2005) The deep feeding system of Vesuvius involved in recent violent strombolian eruptions. Geophysical Research Letters, 32, L02306.
Mazer, J., Bates, J., Stevenson, C., and Bradley, J. (1991) The effect of glass composition on the experimental hydration of obsidian between 110 and 230 °C. Argonne National Laboratory, Illinois.
Métrich, N., and Wallace, P.J. (2008) Volatile abundances in basaltic magmas and their degassing paths tracked by melt inclusions. Reviews in Mineralogy and Geochemistry, 69, 363–402.
Moore, L., Gazel, E., Tuohy, R., Lloyd, A., Esposito, R., Steele-MacInnis, M.J., Hauri, E.H., Wallace, P., Plank, T., and Bodnar, R.J. (2015) Bubbles matter: An assessment of the contribution of vapor bubbles to melt inclusion volatile budgets American Mineralogist, 100, 806–823.
Parruzot, B., Jollivet, P., Rébiscoul, D., and Gin, S. (2015) Long-term alteration of basaltic glass: Mechanisms and rates. Geochimica et Cosmochimica Acta, 154, 28–48.
Redi, D. (2014) Pyroxene and olivine chemistry as an indicator of melt evolution. A contribution to the understanding of Somma-Vesuvius eruptive behaviour, Ph.D. thesis, University of Tasmania and and University of Napoli Federico II.
Robidoux, P., Frezzotti, M.L., Hauri, E.H., and Aiuppa, A. (2015) Low-temperature superficial chemical changes and post-entrapment effects alter CO_2 budget estimation in vapor bubbles of glass inclusions. AGU Meeting 2015, San Francisco, California.
Sobolev, A.V., Dmitriev, L.V., Barsukov, V.L., Nevsorov, V.N., and Slutsky, A.B. (1980) The formation conditions of the high magnesium olivines from the monomineralic fraction of Luna 24 regolith. Proceedings of the Lunar and Planetary Science Conference, 11, 105–116.
Steele-MacInnis, M.J., Esposito, R., and Bodnar, R.J. (2011) Thermodynamic model for the effect of post-entrapment crystallization on the H_2O-CO_2 systematics of volatile saturated silicate melt inclusions. Journal of Petrology, 52, 2461–2482.
Wallace, P.J., Kamenetsky, V.S., and Cervantes, P. (2015) Melt inclusion CO_2 contents, pressures of olivine crystallization, and the problem of shrinkage bubbles. American Mineralogist, 100, 787–794.
Webster, J., Raia, F., De Vivo, B., and Rolandi, G. (2001) The behavior of chlorine and sulfur during differentiation of the Mt. Somma-Vesuvius magmatic system. Mineralogy and Petrology, 73, 177–200.
Yang, K., and Scott, S.D. (1996) Possible contribution of a metal-rich magmatic fluid to a sea-floor hydrothermal system. Nature, 383, 420–423.
Zajacz, Z., Halter, W.E., Pettke, T., and Guillong, M. (2008) Determination of fluid/melt partition coefficients by LA-ICPMS analysis of co-existing fluid and silicate melt inclusions: controls on element partitioning. Geochimica et Cosmochimica Acta, 72, 2169–2197.

Manuscript received January 20, 2016
Manuscript accepted March 17, 2016
Manuscript handled by Ian Swainson